research papers

X-ray investigations of sulfur-containing fungicides. II.[1] Intramolecular forces governing the conformation of four novel α-phenylazo- and α-phenylhydrazono-β-ketosulfones

W. M. Wolf

Institute of General and Ecological Chemistry (I-17), Technical University of Łódź, Żwirki 36, 90-924 Łódź, Poland

Correspondence e-mail: wmwolf@p.lodz.pl

The crystal and molecular structures of four novel β-ketosulfones, phenyl benzoyl(phenylhydrazono)methyl sulfone (I), phenyl benzoyl(4-nitrophenylhydrazono)methyl sulfone (II), (benzoyl)(phenyl)(phenylazo)methyl phenyl sulfone (III) and (benzoyl)(phenyl)(3-chlorophenylazo)-methyl 4-tolyl sulfone (IV), have been investigated using X-ray analysis and density functional theory supplemented by *ab initio* Hartree–Fock calculations. The conformations of (I) and (II) are stabilized by strong intramolecular resonance-assisted hydrogen bonds formed between the sulfonyl and the α-hydrazono moieties. The following increase of a positive charge on the S atoms is compensated *via* π-conjugation and stereoelectronic back-donation from the nearby β-carbonyl group. Compounds (III) and (IV) adopt a strongly distorted propeller shape with pivotal tetrahedral C1 atoms. Distortion mostly follows from the approximate coplanarity of the α-azophenyl and α-phenyl moieties opposite each other. The main stereoelectronic interactions involve the donation of electron density from the α-azo N2 towards the sulfonyl S and the β-carbonyl C2 atoms.

1. Introduction

The present work is part of a larger project aimed at identifying the molecular properties which are responsible for the antimycotic activity of the α-hydrazono- and α-azo-β-keto-sulfones (Wolf, 1999*a*). A previous scheme of intramolecular interactions governing molecular conformation was based solely on the geometrical analysis of 12 X-ray determined structures (Wolf, 1999*b*). Its major shortcoming was that no molecular electronic parameters were taken into consideration. Preliminary experiments have shown that the investigated compounds inhibit the growth of *Alternaria alternata*, *Aspergillus niger* and *Rhisoctonia solani*. In particular, activity is significantly increased after exposing fungi colonies with added fungicide to radiation of daylight characteristics (Zakrzewski & Kacała, 1998; Zakrzewski, 1999, and references therein). The latter can be explained by the slow photodynamic degradation which yields sulfur dioxide and other products which help to destroy the fungal mycelium. Negative charge, present on the fungal cell walls, hinders cationic fungicides passing through and reduces their activity (Hasall, 1982). Therefore, non-cationic fungicides (such as the compounds investigated here or sulfur dioxide) should penetrate the cell walls of most fungi more easily.

The conformation of β-ketosulfones is very often controlled by stereoelectronic effects (Kucsman & Kapovits, 1985;

[1] Part I: Wolf (1999*a*).

Grossert *et al.*, 1987; Dal Colle *et al.*, 1995; Distefano *et al.*, 1996, and references therein). These effects tend to reduce the energy gap between the bonding and non-bonding orbitals of the respective polar bonds and the lone pairs, and very often contribute to the HOMO/LUMO barrier (Graczyk & Mikołajczyk, 1994; Juaristi & Cuevas, 1995; Cramer, 1996). The latter is correlated with the excitation energy and therefore may be regarded as a crude measure of the photodynamic activity (Fleming, 1976).

In this paper the main intramolecular interactions which stabilize the conformation of the four novel α-phenylhydrazono- and α-phenyl-α-phenylazo-β-ketosulfones (I)–(IV) are described. Their crystal structures have been determined by X-ray analysis. Electronic properties of the investigated molecules were calculated at the *ab initio* molecular orbitals level using density functional theory and restricted Hartree–Fock methodologies. The uniform numbering scheme applied to tables and used throughout the discussion is presented here. This scheme differs slightly to that which has been employed during the X-ray structure determinations. The latter is presented in Fig. 1.

(I) $R = H$
(II) $R = NO_2$

(III) $R_1 = H; R_2 = H$
(IV) $R_1 = CH_3; R_2 = Cl$
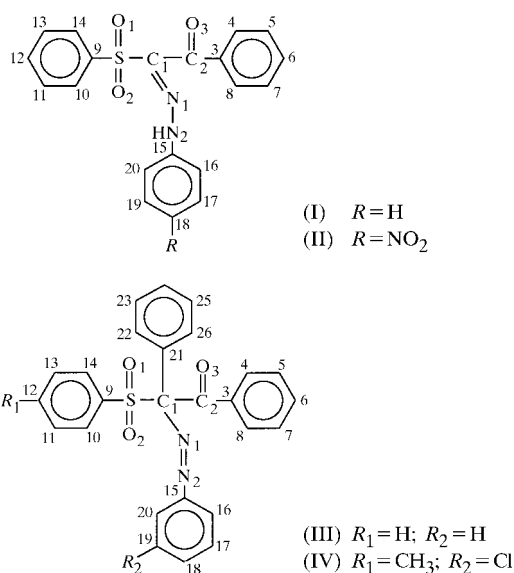
2. Experimental

2.1. Synthesis

The compounds were prepared by Dr A. Zakrzewski at the Department of Technology and Chemical Engineering, Technical and Agricultural Academy, Bydgoszcz, Poland. Compounds (I) and (II) were synthesized by a reaction of benzoylmethyl phenyl sulfone with phenyldiazonium chloride and *p*-nitrodiazonium chloride, respectively. Compound (III) was synthesized using benzoylphenylmethyl phenyl sulfone and phenyldiazonium chloride, while (IV) was made using benzoylphenylmethyl *p*-tolyl sulfone and *m*-chlorophenyldiazonium chloride. All the above reactions were carried out in alkaline ethyl alcohol solutions (Zakrzewski, 1996).

2.2. X-ray crystallography

Crystals of (I), (III) and (IV) were obtained by vapour diffusion. A sample of (I) dissolved in methanol was equilibrated against pure isopropanol for 2 weeks. Compounds (III) and (IV) were dissolved in a 3:1 mixture of chloroform and isopropanol and equilibrated against pure isopropanol for 12 and 6 d, respectively. All the crystallizations described above were performed at room temperature. Crystals of (II) were grown in a hot box from the almost saturated methanol solution over 2 d; the starting temperature was approximately 323 K.

Details of crystal symmetry, data collections, structure determinations and refinements are summarized in Table 1.[2] All non-H atoms were located on E maps. The H atoms of all the compounds were routinely located in difference Fourier maps calculated after three cycles of an anisotropic refinement. Their positional and isotropic displacement parameters were allowed to refine freely. In (II) the diffraction data with $2\theta > 150°$ and one reflection ($-1,0,1$) identified as an outlier were not used in the final refinement. All data were used for the remaining three crystals.

Standard bond lengths quoted throughout the paper have been taken from the *International Tables for Crystallography* (Allen *et al.*, 1992). Hammett's σ_p constants were obtained from Hansch & Leo (1979) and van der Waals' radii from Bondi (1964).

The interactive molecular graphics programs *SYBYL* (TRIPOS Associates Inc., 1996) and *XP* (Siemens, 1990) were used for analysis of molecular geometry and the preparation of drawings.

2.3. Molecular orbital calculations

The molecular structures of the investigated compounds were optimized and Mayer's bond orders (Mayer, 1986) were calculated using the DFT (density functional theory) formalism (Hohenberg & Kohn, 1964; Levy, 1979), as implemented in DMOL (Molecular Simulations Inc., 1996). The DNP double-zeta quality basis set (equivalent to the 6-31G**) and the gradient-corrected correlation functionals BLYP (Lee *et al.*, 1988) have been applied. For comparison, (I) has also been optimized using the 6-31+G(d) basis set, *i.e.* a split-valence 6-31G basis set additionally augmented by a set of diffuse functions and the B3LYP hybrid exchange-correlation functional (Becke, 1993). The final molecular electronic properties were calculated in a single point using the restricted Hartree–Fock (RHF) method and the triple zeta 6-311+G(d,p) basis set. Atomic charges were calculated to fit the electrostatic potential at points selected accordingly to the Merz–Singh–Kollman scheme (Besler *et al.*, 1990; Singh & Kollman, 1984). The B3LYP geometry optimization and the single point calculations were performed with the *GAUSSIAN*98 suite of programs (Frisch *et al.*, 1998).

---

[2] Supplementary data for this paper are available from the IUCr electronic archives (Reference: OS0056). Services for accessing these data are described at the back of the journal.

3. Results and discussion

A view of the compounds investigated with the atom-numbering scheme used in the X-ray structure determinations is shown in Fig. 1. Selected geometrical parameters accompanied by results of the DFT geometry optimizations are given in Tables 2 and 3. Electrostatic atomic charges and selected molecular electronic properties are shown in Table 4.

3.1. Molecular structure of (I) and (II)

In the crystal structures the S=O2 sulfonyl double bonds, carbonyl groups and phenylhydrazone fragments are approximately coplanar. The molecular conformations of these fragments are similar to those observed in 4′-{[benzoyl(4-tolylhydrazono)methyl]sulfonyl}acetanilide (V) (Wolf, 1999b). Similar conformations have been observed in β-ketoarylhydrazones (Bertolasi, Nanni et al., 1994) and were defined as EZE. This three-letter symbol was initially used to describe the conformation of 2,2-diacylethenamines (Gómez-Sánchez et al., 1987). In (I), (II) and (V), these three letters indicate the positions of the carbonyl C2=O3, the sulfonyl S=O2 double bonds as well as the N2—C15 bonds bearing the aryl substituent relative to the C1=N1 bond. Planar central fragments of the molecules are stabilized by the strong, cyclic intramolecular hydrogen bonds assisted by resonance connecting the hydrazone and sulfone moieties, see Table 5 for details.

The semi-empirical model of resonance-assisted hydrogen bonding (RAHB) has been formulated by Gilli et al. (1989). Strong intramolecular RAHBs have been identified in

β-diketone enols (Bertolasi et al., 1991) and β-diketoarylhydrazones (Bertolasi, Gilli et al., 1994). In the latter compounds the strength of the intramolecular RAHB is mainly related to the degree of π-delocalization existing in the C=N—N fragment of a molecule and modulated by the inductive and non-bonding interactions. In particular, Bertolasi et al. (1993) have found that in compounds similar to (VI) the electron-withdrawing substituents X borne by the phenyl ring bonded to the hydrazone N atoms tend to reduce the strength of the RAHB, while the electron-donating substituents act in the opposite direction.

(VI)
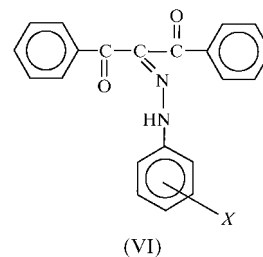
The almost ideal planarity of the six-membered RAHB rings suggests a high level of π-delocalization. However, the X-ray determined S—C1 bond lengths [1.784 (1) and 1.798 (2) Å in (I) and (II), respectively] are larger than values reported both for the Csp^2—S single bonds (1.751 Å) and for the Csp^3—SO_2 bonds (1.779 Å). The N1=C1 bonds [1.302 (2) and 1.298 (3) Å in (I) and (II), respectively] are close to those reported for the S—C=N—X system (1.302 Å), but longer than similar bonds found in the C—C=N—C moiety (1.279 Å). The N1—N2 bond in (I) [1.303 (2) Å] is slightly shorter than the similar bond in (II) [1.315 (3) Å]. Both bonds are longer than the typical N=N double bond (1.240 Å), much shorter than planar N—N single bonds (1.401 Å) and close to the partially double aromatic nitrogen–nitrogen bonds, 1.304 Å. The S—C1 Mayer's bond orders (see Table 6 for the details) in (I) and (II) are practically the same (1.11 and 1.10, respectively) and indicate that the influence of the strongly electron-withdrawing phenylsulfonyl group (Hammett's constant, $\sigma_p = 0.70$) is based on inductive rather than conjugation effects. However, analysis of bond orders in the C1=N1—N2 fragment shows, as suggested by the bond length comparison presented above, a slightly higher level of π-conjugation in (I) than in (II). The N1=C1 bond orders are 1.59 and 1.62,
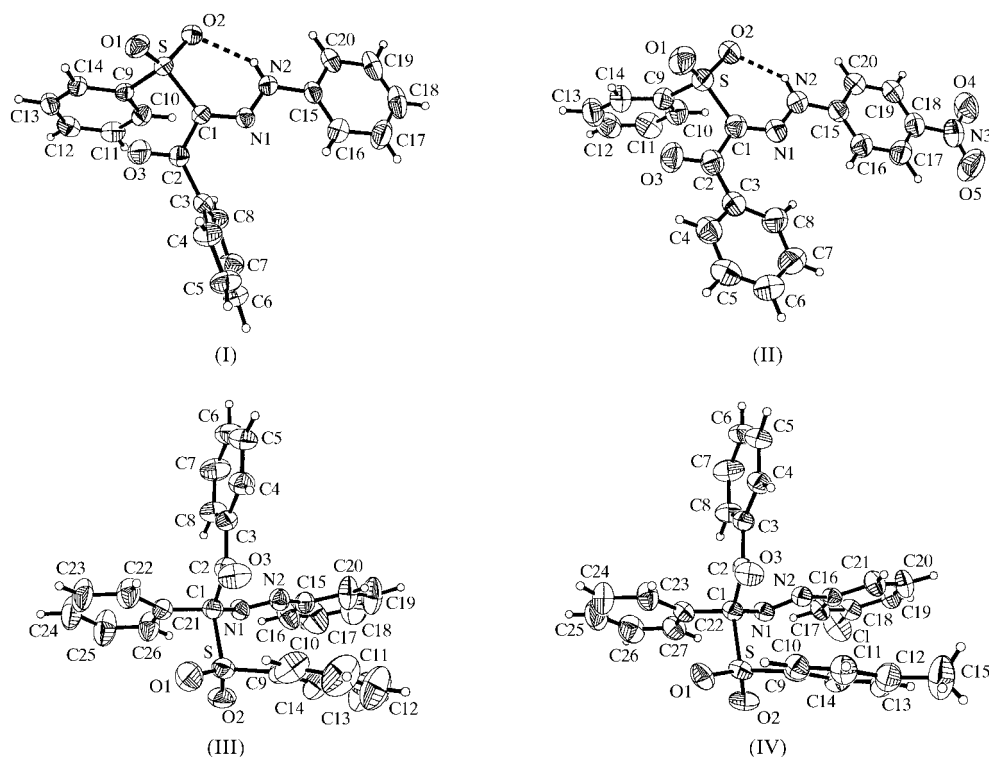
Figure 1
View of the compounds investgated, with atom labels which were used during the X-ray structure determinations.

Table 1
Experimental details.

	(I)	(II)	(III)	(IV)
Crystal data				
Chemical formula	$C_{20}H_{16}N_2O_3S$	$C_{20}H_{15}N_3O_5S$	$C_{26}H_{20}N_2O_3S$	$C_{27}H_{21}ClN_2O_3S$
Chemical formula weight	364.43	409.41	440.5	488.97
Cell setting, space group	Triclinic, $P\bar{1}$	Monoclinic, $P2_1/n$	Monoclinic, $P2_1/c$	Monoclinic, $P2_1/c$
a, b, c (Å)	5.6784 (7), 11.3204 (15), 14.1087 (19)	14.8351 (7), 6.0456 (5), 21.0161 (12)	13.285 (3), 16.577 (3), 11.421 (2)	14.155 (2), 9.542 (1), 18.822 (1)
α, β, γ (°)	102.441 (11), 97.544 (10), 97.447 (11)	90, 98.613 (6), 90	90, 114.80 (3), 90	90, 109.820 (9), 90
V (Å³)	866.1 (2)	1863.6 (2)	2283.2 (8)	2391.6 (4)
Z	2	4	4	4
D_x (Mg m^{-3})	1.397	1.459	1.281	1.358
Radiation type	Mo $K\alpha$	Cu $K\alpha$	Mo $K\alpha$	Mo $K\alpha$
No. of reflections for cell parameters	48	82	48	26
θ range (°)	4.7–17.3	9–15	5–13.5	4.7–12.0
μ (mm^{-1})	0.210	1.892	0.172	0.279
Temperature (K)	290 (2)	292 (2)	291 (2)	291 (2)
Crystal form, colour	Approximately sphere shaped, pale yellow	Prism, pale yellow	Prism, yellow	Prism, yellow
Crystal size (mm)	$0.25 \times 0.23 \times 0.21$	$0.42 \times 0.21 \times 0.12$	$0.45 \times 0.40 \times 0.25$	$0.40 \times 0.30 \times 0.15$
Crystal radius (mm)	–	0.25	–	–
Data collection				
Diffractometer	Siemens P3	Kuma Diffraction KM-4	Siemens P3	Siemens P3
Data collection method	ω–2θ scans	ω–2θ scans	ω–2θ scans	ω–2θ scans
Absorption correction	None	ψ-scan	None	None
T_{min}	–	0.445	–	–
T_{max}	–	0.797	–	–
No. of measured, independent, observed reflections	5669, 4010, 3221	4566, 3710, 2943	6194, 5156, 3703	6942, 5538, 3727
Criterion for observed reflections	$I > 2\sigma(I)$	$I > 2\sigma(I)$	$I > 2\sigma(I)$	$I > 2\sigma(I)$
R_{int}	0.0565	0.0204	0.0329	0.0284
θ_{max} (°)	27.56	74.91	27.56	27.56
Range of h, k, l	$-2 \rightarrow h \rightarrow 7$ $-14 \rightarrow k \rightarrow 14$ $-18 \rightarrow l \rightarrow 18$	$-18 \rightarrow h \rightarrow 18$ $-1 \rightarrow k \rightarrow 7$ $0 \rightarrow l \rightarrow 26$	$-1 \rightarrow h \rightarrow 17$ $-21 \rightarrow k \rightarrow 1$ $-14 \rightarrow l \rightarrow 13$	$-1 \rightarrow h \rightarrow 18$ $-1 \rightarrow k \rightarrow 12$ $-24 \rightarrow l \rightarrow 23$
No. and frequency of standard reflections	3 every 97 reflections	3 every 100 reflections	3, every 97 reflections	3, every 97 reflections
Intensity decay (%)	3	5	5	3
Refinement				
Refinement on	F^2	F^2	F^2	F^2
$R[F^2>2\sigma(F^2)], wR(F^2), S$	0.0362, 0.0973, 1.030	0.0488, 0.1459, 0.932	0.0482, 0.1371, 1.028	0.0411, 0.1102, 0.968
No. of reflections and parameters used in refinement	4010, 300	3710, 323	5156, 366	5538, 392
H-atom treatment	All H-atom parameters refined	All H-atom parameters refined	All H-atom parameters refined	All H-atom parameters refined
Weighting scheme	$w = 1/[\sigma^2(F_o^2) + (0.0457P)^2 + 0.2341P]$, where $P = (F_o^2 + 2F_c^2)/3$	$w = 1/[\sigma^2(F_o^2) + (0.0759P)^2 + 1.2875P]$, where $P = (F_o^2 + 2F_c^2)/3$	$w = 1/[\sigma^2(F_o^2) + (0.0790P)^2 + 0.2414P]$, where $P = (F_o^2 + 2F_c^2)/3$	$w = 1/[\sigma^2(F_o^2) + (0.0623P)^2]$, where $P = (F_o^2 + 2F_c^2)/3$
$(\Delta/\sigma)_{max}$	0.003	0.007	0.010	0.012
$\Delta\rho_{max}, \Delta\rho_{min}$ (e Å^{-3})	0.389, −0.371	0.331, −0.488	0.543, −0.312	0.286, −0.272
Extinction method	$SHELXL$ (Sheldrick, 1997a)	$SHELXL$ (Sheldrick, 1997a)	None	$SHELXL$ (Sheldrick, 1997a)
Extinction coefficient	0.020 (2)	0.0019 (3)	–	0.0026 (6)

† Computer programs used: $P3$ (Siemens, 1989), KM-4 (Kuma Diffraction, 1991), $XDISK$ (Siemens, 1991), $DATAPROC$9.0 (Gałdecki *et al.*, 1995), $SHELXS$97 (Sheldrick, 1997b).

while N1═N2 bond orders are 1.36 and 1.32 for (I) and (II), respectively.

The influence of the electron-withdrawing *p*-nitrophenyl group attached to the hydrazone moiety in (II), as compared to the almost neutral phenyl group in (I) (Hammett's σ_p constants are 0.23 and −0.01, respectively), extends further than the hydrazone region. The Merz–Singh–Kollman atomic charge distribution within the N1═N2—C1 fragment is more uniform in (II) than in (I), see Table 4 for details. On the other

hand, the already large positive charge located on the sulfur atom in (I) is even greater in (II) (1.115 and 1.253 e, respectively). Similarly, the negative charge on the O2 atom involved in the RAHB is slightly larger in (II) than in (I), −0.684 and −0.650 e, respectively. The hydrazone H2 atoms are stripped of electron density in (II) more than in (I). The positive charges are 0.335 and 0.265 e, respectively. Subsequently, H atoms in (II) are more attracted by the sulfonyl O2 atoms and form stronger intramolecular O2$\cdots$H2—N2 hydrogen bonds.

Table 2
Selected geometrical parameters of (I) and (II), as determined by X-ray analysis and accompanied by the DFT geometry optimization results.

	(I)			(II)	
	X-ray	BLYP/DNP	B3LYP/ 6-31+G(d)	X-ray	BLYP/DNP
Selected bond lengths (Å)					
S=O1	1.431 (1)	1.468	1.457	1.435 (2)	1.466
S=O2	1.444 (1)	1.493	1.476	1.446 (2)	1.491
S—C1	1.784 (1)	1.852	1.821	1.798 (2)	1.884
S—C9	1.765 (2)	1.819	1.782	1.759 (2)	1.824
N1=C1	1.302 (2)	1.311	1.301	1.298 (3)	1.309
N1—N2	1.303 (2)	1.316	1.306	1.315 (3)	1.327
N2—C15	1.402 (2)	1.418	1.409	1.397 (3)	1.405
C1—C2	1.476 (2)	1.487	1.484	1.492 (3)	1.494
C2=O3	1.220 (2)	1.241	1.227	1.220 (3)	1.243
C2—C3	1.491 (2)	1.508	1.499	1.492 (4)	1.509
Selected intramolecular non-bonding distances (Å)†					
S···O3 [3.32]	2.976 (1)	2.957	2.957	2.818 (3)	2.847
O1···C2 [3.22]	3.220 (1)	3.261	3.250	3.158 (3)	3.309
S···N2 [3.35]	3.107 (2)	3.158	3.101	3.102 (3)	3.122
O2···N1 [3.07]	2.969 (2)	2.937	2.917	2.959 (3)	2.963
O2···N2 [3.07]	2.668 (2)	2.642	2.596	2.642 (3)	2.596
Selected torsion angles (°)					
α: S—C1—C2—O3	−17.8 (2)	−4.8	−11.4	7.2 (3)	5.4
α': S—C1—N1—N2	2.3 (2)	−4.5	−4.3	−1.6 (3)	−4.6
β: O1—S—C1—C2	53.6 (1)	63.2	56.8	54.9 (2)	61.9
β': O1—S—C1—N1	−127.3 (1)	−109.3	−114.9	−124.5 (2)	−113.1
γ: O2—S—C1—C2	−176.7 (1)	−167.9	−174.9	−177.0 (2)	−170.6
γ': O2—S—C1—N1	2.5 (1)	16.6	13.3	3.5 (2)	14.4
C1—C2—C3—C4	135.2 (2)	139.5	148.4	161.9 (2)	169.7

† Accompanied by the corresponding sums of the van der Waal's radii (Å), given in square brackets.

respect to the negative sulfonyl O1 atoms, at a distance [3.220 (2) and 3.158 (3) Å, respectively], equal or smaller to the sum of the respective van der Waals radii, 3.22 Å.

A similar pattern of non-bonding interactions has been reported by Distefano *et al.* (1991, 1996) in a series of papers concerned with the intramolecular interactions in mostly α,α-unsubstituted β-carbonyl sulfones and sulfoxides (Dal Colle *et al.*, 1995). In these compounds the highly polar C_α—S bonds were located *gauche* with respect to the β-carbonyl groups permitting the mutual hyperconjugative (Hoffmann, 1971) $\pi_{C=O} - \sigma^*_{C-S}$ and $\pi^*_{C=O} - \sigma_{C-S}$ interactions. Intensive electrostatic charge transfers from the negatively charged β-carbonyl and sulfonyl O atoms towards the strongly positive sulfur and β-carbonyl C atoms were also detected by the UV photo-electron spectroscopy supported by the molecular quantum mechanic calculations. Therefore, the shortening of the S···O(3) and O(1)···C(2) non-bonding distances with respect to the sum of the van der Waals radii could be used as a rough measure of stereoelectronic interactions.

The latter is also supported by the slightly higher Mayer's O2···H2 bond orders (0.21 and 0.19) and shorter O2···N2 distances, as determined by X-ray analysis. The latter are 2.642 (3) and 2.668 (2) Å in (II) and (I), respectively. Using the electrostatic potential derived atomic charges to estimate the strength of the heteronuclear hydrogen bonds seems to be justified in view of the recent Gilli's *et al.* (1994) conclusion that such bonds are mostly of electrostatic nature.
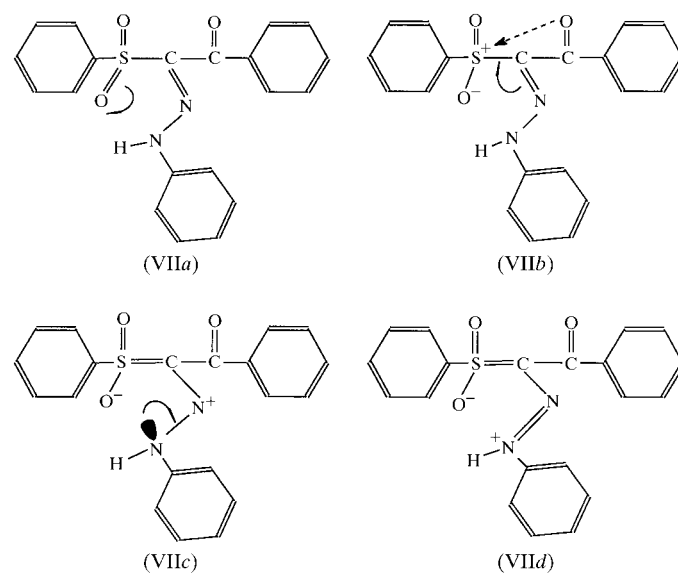
Aromatic rings directly bonded to the hydrazone moieties are approximately coplanar with the RAHB cyclic systems. The N2—C15 bond lengths in (I) and (II) are practically the same [1.402 (2) and 1.397 (3) Å, respectively] and smaller than the typical C—N bond length reported for the C_{ar}—N=N fragment (1.431 Å). Mayer's bond orders are very similar (1.23 and 1.24, respectively). However, opposite to above parameters, both phenyl rings do not show significant quinoid character, as indicated by an examination of the respective bond lengths and angles. Therefore, the influence of the *p*-nitrophenyl group in (II) as compared to the unsubstituted phenyl ring in (I) is based on inductive, rather than π-delocalization effects.

In (I) and (II) the negatively charged carbonyl O3 atoms are positioned closer to the highly positive S atoms [2.976 (1) and 2.818 (3) Å, respectively] than the sum of the sulfur and oxygen van der Waals radii, 3.32 Å. Carbonyl C2 atoms bearing the substantial positive charge are situated, with

(VIIa)

(VIIb)

(VIIc)

(VIId)

In (I) and (II) the intramolecular hydrogen bonds increase the semi-polar character of the sulfur=oxygen double bonds and prompt the electron density to be partially transferred

Table 3
Selected geometrical parameters of (III) and (IV), as determined by X-ray analysis and accompanied by the DFT geometry optimization results.

	(III)		(IV)	
	X-ray	BLYP/DNP	X-ray	BLYP/DNP
S=O1	1.420 (2)	1.470	1.430 (1)	1.469
S=O2	1.432 (2)	1.473	1.437 (1)	1.474
S−C1	1.878 (2)	2.012	1.885 (2)	2.002
S−C9	1.763 (2)	1.834	1.766 (2)	1.826
N1−C1	1.476 (2)	1.465	1.479 (2)	1.466
N1=N2	1.243 (2)	1.278	1.247 (2)	1.282
N2−C15 [C16 for (IV)]	1.425 (2)	1.435	1.430 (2)	1.431
C1−C2	1.538 (2)	1.563	1.545 (2)	1.568
C1−C21 [C22 for (IV)]	1.521 (2)	1.519	1.515 (2)	1.521
C2=O3	1.211 (2)	1.228	1.210 (2)	1.227
C2−C3	1.481 (2)	1.515	1.493 (2)	1.517
Selected intramolecular non-bonding distances (Å)†				
S···O3 [3.32]	2.910 (2)	3.042	2.945 (2)	3.031
O1···C2 [3.22]	3.271 (2)	3.337	3.290 (2)	3.306
S···N2 [3.35]	3.150 (2)	3.264	3.234 (2)	3.312
O2···N1 [3.07]	2.773 (2)	2.891	2.802 (2)	2.935
O2···N2 [3.07]	3.408 (2)	3.638	3.522 (2)	3.739
N2···C2 [3.25]	2.701 (2)	2.706	2.623 (2)	2.617
Selected torsion angles (°)				
α: S−C1−C2−O3	−10.6 (2)	−2.9	−8.6 (2)	−4.9
α': S−C1−N1−N2	−82.9 (2)	−87.5	−89.3 (1)	−91.7
β: O1−S−C1−C2	68.1 (1)	61.4	69.2 (1)	62.4
β': O1−S−C1−N1	−168.7 (1)	−176.8	−168.6 (1)	−177.3
β'': O1−S−C1−C21 [C22 for (IV)]	−52.9 (1)	−59.8	−51.9 (1)	−57.4
γ: O2−S−C1−C2	−164.7 (1)	−169.9	−163.2 (1)	−168.9
γ': O2−S−C1−N1	−41.6 (1)	−48.1	−41.1 (1)	−48.6
γ'': O2−S−C1−C21 [C22 for (IV)]	74.2 (1)	69.0	75.6 (1)	71.3
Valency angles (°) defining coordination spheres of the pivotal C1 atoms				
S−C1−N1	104.6 (1)	101.6	105.2 (1)	102.5
S−C1−C2	111.4 (1)	110.7	111.7 (1)	110.6
S−C1−C21 [C22 for (IV)]	104.4 (1)	99.9	104.0 (1)	101.5
N1−C1−C2	113.6 (1)	114.3	112.3 (1)	112.6
N1−C1−C21 [C22 for (IV)]	110.2 (1)	113.8	110.9 (1)	115.7
C2−C1−C21 [C22 for (IV)]	111.9 (1)	114.6	112.1 (1)	112.7

† Accompanied by corresponding sums of the van der Waal's radii (Å), given in square brackets.

from the S towards the O2 atoms, as shown in (VII*b*). The following increase of the positive charge on sulfur can be compensated *via* the π-conjugation as in (VII*c*) and (VII*d*) or by the stereoelectronic back-donation from the nearby β-carbonyl group, as indicated by an arrow in (VII*b*). Both mechanisms take place in (I) and (II). However, in the latter compound the electron-withdrawing *p*-nitrophenyl group attached to the hydrazone moiety destabilizes canonical structures with the positive charge located on the N atoms to a larger extent than the almost neutral phenyl group in (I). This effect intensifies the stereoelectronic charge transfer from the β-carbonyl towards the sulfonyl group and furthermore strengthens the intramolecular RAHB in (II) compared with (I). Similar anomeric back-donation of the electron density triggered by the hydrogen-bond formation has recently been identified in aminals by Alder *et al.* (1999).

The S−C1 bonds are positioned *syn* with respect to the carbonyl C2=O3 group. This suggests that hyperconjugation is substantially weaker than in *gauche* conformers of the α,α-unsubstituted β-carbonyl sulfones and the stereoelectronic charge transfer is mostly of electrostatic origin. However, in view of reports on the *syn*-anomeric effect (Graczyk & Mikołajczyk, 1994; Juaristi & Cuevas, 1995, and references quoted therein), the former contribution of hyperconjugative interactions cannot be completely ruled out. Quite recently Olivato *et al.* (1998, 2000) presented a multidisciplinary study of β-carbonyl sulfoxides, in which they have shown that, similarly to the investigated compounds (I) and (II), the *syn* configuration of S−C_α and C=O bonds is stabilized by Coulombic and intramolecular charge-transfer interactions between the opposite charged atoms of the C=O and S=O dipoles.

The terminal benzoyl phenyl ring in (I) is more twisted with respect to the central planar part of the molecule than in (II). Both rings are very regular and show no resemblence to quinoid structure. Also the C2−C3 bond lengths in (I) and (II) are virtually the same: 1.491 (2) and 1.492 (4) Å, respectively. This suggests that these phenyl rings are not involved in electron-density delocalizations and their positions are fixed by the weak non-bonding van der Waals interactions.

3.2. Molecular structure of (III) and (IV)

Compounds (III) and (IV) adopt a strongly distorted propeller shape with the pivotal tetrahedral C(1) atoms. Distortion mostly follows from the approximate coplanarity of the oppositely located α-azophenyl and α-phenyl moieties.

Examination of dihedral angles as specified in Table 3 clearly shows that the X-ray determined as well as the DFT-minimized conformations of (III) and (IV) generate a large number of *cis* and *gauche* interactions involving the highly polar sulfonyl, α-azo and β-carbonyl groups. All these groups incorporate electronegative N and O atoms bearing non-bonding lone pairs. The highly positive S atoms (see Table 4 for the atomic charges) are located closer to the neighbouring carbonyl O3 and the azo N2 atoms bearing negative charge than the sum of S···O and S···N van der Waals radii. Also, the

Table 4
Selected Merz–Singh–Kollman electrostatic atomic charges (e), overall Hartree–Fock molecular energy (H), dipole moments (D), HOMO and LUMO energies (eV) calculated at the HF/6-311+G(d,p) level.

	(I)	(II)	(III)	(IV)
S	1.115	1.253	1.261	1.181
O1	−0.591	−0.617	−0.622	−0.618
O2	−0.650	−0.684	−0.627	−0.637
O3	−0.503	−0.504	−0.424	−0.413
N1	−0.310	−0.130	−0.240	−0.267
N2	−0.054	−0.190	−0.135	−0.154
H2	0.265	0.335	–	–
C1	0.137	−0.095	−0.256	0.136
C2	0.343	0.512	0.362	0.158
C3	0.165	−0.092	−0.165	0.113
C9	−0.082	−0.107	−0.241	−0.180
C15	0.225	0.269	0.430	0.194
C21	–	–	0.360	0.238
E(HF)	−1497.58	−1701.13	−1726.95	−2224.99
D_m	6.79	5.95	6.76	7.31
HOMO	−8.506	−9.361	−9.083	−9.031
LUMO	0.121	0.378	1.211	0.950

Table 5
The resonance-assisted intramolecular hydrogen-bond parameters in (I) and (II), as determined by an X-ray analysis and accompanied by the DFT geometry optimization results.

	(I)			(II)	
	X-ray	BLYP/ DNP	B3LYP/ 6-31+G(d)	X-ray	BLYP/ DNP
N2—H2 (Å)	0.84 (2)	1.06	1.03	0.89 (3)	1.06
O2···H2 (Å)	1.98 (2)	1.788	1.76	1.92 (2)	1.685
O2···H2—N2 (°)	136.6 (1)	135.0	136.0	136.9 (1.6)	141.1
O2···N2 (Å)	2.668 (2)	2.642	2.596	2.642 (2)	2.596
d† (Å)	0.02	0.12	0.06	0.01	0.07

† RMS (root mean square) deviation from the least-squares optimized O2, S, C1, N1, N2, H2 mean plane.

positively charged C2 atoms of the β-carbonyl groups form short intramolecular contacts to the sulfonyl O1 and the azo N2 atoms. Details on interatomic distances accompanied by the corresponding van der Waals radii are summarized in Table 3. This suggests that the pattern of stereoelectronic interactions in (III) and (IV) is more complicated than in (I) and (II). It can be conveniently characterized using the concept of the 'double bond – no bond resonance' initially introduced by Brockway (1937) and Roberts *et al.* (1950), and further widely applied to the visualization of an anomeric effect (Graczyk & Mikołajczyk, 1994; Juaristi & Cuevas, 1995, and references therein). In addition to the interactions already described in (I) and (II), and involving the sulfonyl and the β-carbonyl groups, represented by canonical structures (VIII*b*) and (VIII*c*), the α-azo moieties can also participate in the stereoelectronic charge transfer as indicated by (VIII*d*) and (VIII*e*).

Important evidence of stereoelectronic interactions are unusual S—C1 bonds [1.878 (2) and 1.885 (2) Å in the X-ray structures of (III) and (IV), respectively], which are much longer than the normally observed single carbon–sulfur bond, 1.78 Å. Analysis of non-bonding intramolecular distances

indicates that the steric strain induced deformations (such as those described by Rüchardt & Beckhaus, 1985) cannot be a major reason for the elongation of S—C1 bonds. This suggests that the real molecules are to a larger extent represented by canonical structures with the broken S—C1 bond, *i.e.* (VIII*b*) and (VIII*d*) than by (VIII*c*), in which S—C1 is a double bond. However, the C1—C2 bonds [1.538 (2) and 1.545 (2) Å in the X-ray structures of (III) and (IV), respectively] are longer than the single carbon–carbon bonds, as found in aliphatic ketones C—C(O)—C (1.511 Å), and suggests that the contribution of structure (VIII*b*) with the double C1—C2 bond is less significant.

(VIII*a*)   (VIII*b*)   (VIII*c*)   (VIII*d*)   (VIII*e*)
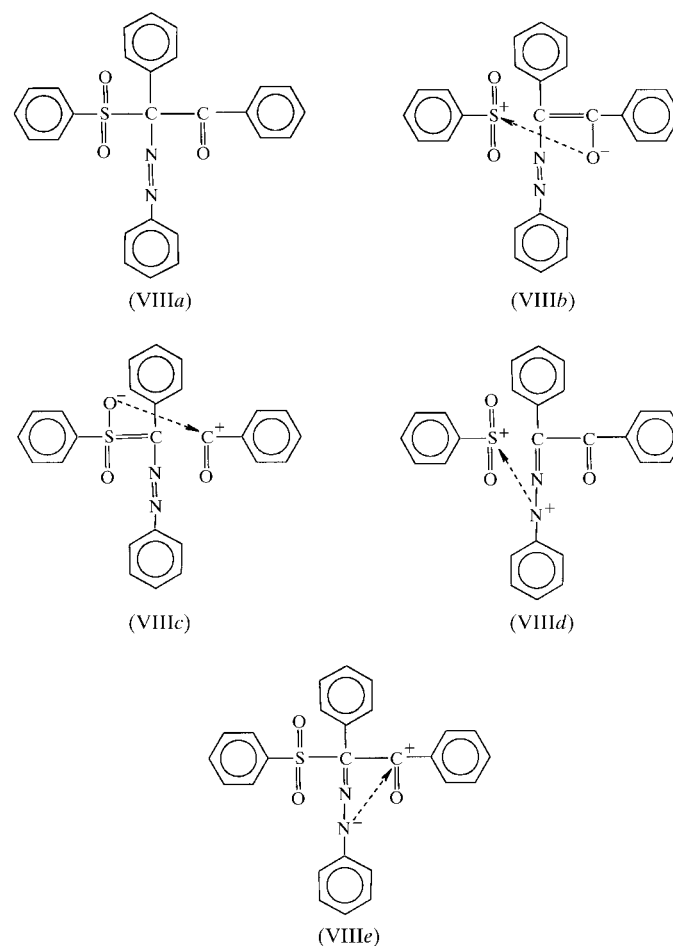
This simple analysis leads to the conclusion that the main stereoelectronic interactions are represented by structures (VIII*d*) and (VIII*e*) and involve the donation of electron density from the azo N2 towards the S and C2 atoms. The latter two structures may be additionally stabilized by conjugation of the α-phenyl ring directly bonded to the C1 atom with the C1—N1 double bond. It explains the odd conformation of (III) and (IV) in which the α-phenylazo fragments are roughly coplanar with the oppositely located α-phenyl rings. The coordination spheres around the C1 atoms are deformed in such a manner that the S—C1—N1 and S—C1—C21 bond angles are significantly smaller than the remaining four angles, Table 3. Considering steric interactions, the phenylsulfonyl group is the largest of all the substituents

bonded to C1. Therefore, in contrast to the results of the X-ray structure determination, all three bond angles involving the S atoms should be larger or at least equal to the remaining three angles. The existing deformation accounts for the significant contribution of resonance structure (VIII*d*) with the N1—C1 double and C1—C2 single bonds accompanied by the broken C1—S bond. In this structure the bond angles N1—C1—C2, N1—C1—C21 and C2—C1—C21 should adopt values close to 120°. The larger S—C1—C2 angle observed may result from the electrostatic repulsion between the negatively charged O atoms of the sulfonyl and carbonyl groups. Indeed, in the X-ray structures of (III) and (IV) the intramolecular non-bonding O1···O3 distances [3.015 (3) and 3.077 (2) Å, in (III) and (IV), respectively] are very close to the sum of the corresponding van der Waals radii, 3.04 Å. Therefore, the contribution of (VIII*e*) should be less significant than that of (VIII*d*) and donation of the electron density from N2 to the S atoms seems to be the dominating stereoelectronic interaction in (III) and (IV). On the other hand, Mayer's bond orders of the C1—C2 bonds are the same in (III) and (IV) (equal to 0.92) and smaller than those of the S—C1 bonds (0.97 and 0.96, respectively). This suggest that (VIII*e*) cannot be completely ruled out. Anomeric interactions represented by the 'double bond – no bond resonance' structures (VIII*b*)–(VIII*e*) increase the charge separation within the molecule. They are accompanied by the Coulombic electrostatic attraction of atoms bearing opposite charges. The latter, indicated by arrows in (VIII*b*)–(VIII*e*), are mostly responsible for the number of short intramolecular distances existing in (III) and (IV).

Contrary to the S—C1 bonds, in all compounds (I)–(IV) the S—C9 bond lengths determined by X-ray analysis are very similar: 1.765 (2), 1.759 (2), 1.763 (2) and 1.766 (2) Å, respectively. They all are very close to a value reported for the single S—C bond found in the C_{ar}—SO_2—C systems, 1.763 Å. Also Mayer's bond orders are practically the same: 1.14, 1.15, 1.14 and 1.14, respectively. This suggests that the terminal phenyl moieties borne by the sulfonyl groups are not involved in stereoelectronic interactions.

4. Conclusions

Comparison of the crystallographic and quantum chemical calculations suggests that the conformations of (I)–(IV) are influenced by stereoelectronic interactions. These effects induce a number of short intramolecular contacts between the sulfonyl, α-azo and β-carbonyl groups. The Merz–Singh–Kollman electrostatic charge distribution, calculated at the HF/6-311+G(d,p) level, clearly shows that the largest positive charge is located on S atoms and indicates that sulfur is the best acceptor of the stereoelectronic electron-density back-donation from neighbouring negatively charged atoms. The latter partially counteracts the strong electron-withdrawing capacity of the sulfonyl group. Similar interactions have been recently observed by Distefano *et al.* (1996) and Olivato *et al.* (1998, 2000). They have found that in α-alkylsulfinylaceto-phenones the cis_1 conformation in the solid state was stabi-

Table 6
Mayers's bond orders of selected bonds as calculated at the BLYP/DNP level.

	(I)	(II)	(III)	(IV)
S—O1	1.87	1.86	1.89	1.89
S—O2	1.77	1.75	1.88	1.87
S—C1	1.11	1.10	0.97	0.96
S—C9	1.14	1.15	1.14	1.14
C1—C2	1.05	1.02	0.92	0.92
C1—C21	–	–	0.96	0.96
C2—C3	1.01	1.05	1.05	1.04
C2—O3	1.87	1.81	1.87	1.88
N1—C1	1.59	1.62	1.04	1.05
N1—N2	1.36	1.32	1.87	1.87
N2—C15	1.23	1.24	1.12	1.12
N2—H2	0.72	0.69	–	–
O2···H2	0.19	0.21	–	–

lized by the Coulombic attraction coupled with the intramolecular charge transfer between negatively charged carbonyl O and positively charged sulfinyl S atoms. The DFT optimized and the X-ray determined structures are similar, the main difference being lengthening (in comparison with the X-ray determined structures) of polar bonds as well as the intramolecular non-bonding distances affected by stereoelectronic effects in the DFT minimized molecules. This elongation reduces steric strain and therefore can lead to an underestimation of the stereoelectronic interactions in the DFT optimized species. The planarity of the six-membered ring closed by the resonance-assisted hydrogen bonds formed between the sulfonyl and α-hydrazono moieties in (I) and (II) is better preserved in the X-ray determined structures than in their DFT minimized analogues.

References

Alder, R. W., Carniero, T. M. G., Mowlam, R. W., Orpen, G., Petillo, P. A., Vachon, D. J., Weisman, G. R. & White, J. M. (1999). *J. Chem. Soc. Perkin Trans. 2*, pp. 589–599.
Allen, F. H., Kennard, O., Watson, D. G., Brammer, L., Orpen, A. G. & Taylor, R. (1992). *International Tables for Crystallography*, edited by A. J. C. Wilson, Vol. C, pp. 691–705. Dordrecht: Kluwer Academic Publishers.
Becke, A. D. (1993). *J. Chem. Phys.* **98**, 5648–5652.
Bertolasi, V., Ferretti, V., Gilli, P., Gilli, G., Issa, Y. M. & Sherif, O. E. (1993). *J. Chem. Soc. Perkin Trans. 2*, pp. 2223–2228.
Bertolasi, V., Gilli, P., Ferretti, V. & Gilli, G. (1991). *J. Am. Chem. Soc.* **113**, 4917–4925.
Bertolasi, V., Gilli, P., Ferretti, V. & Gilli, G. (1994). *Acta Cryst.* B**50**, 617–625.
Bertolasi, V., Nanni, L., Gilli, P., Ferretti, V., Gilli, G., Issa, Y. M. & Sherif, O. E. (1994). *New J. Chem.* **18**, 251–261.

Besler, B. H., Merz Jr, K. M. & Kollman, P. A. (1990). *J. Comput. Chem.* **11**, 431–439.

Bondi, A. (1964). *J. Phys. Chem.* **68**, 441–451.

Brockway, L. O. (1937). *J. Phys. Chem.* **41**, 185–195.

Cramer, J. C. (1996). *J. Mol. Struct. (Theochem.)* **370**, 135–146.

Dal Colle, M., Bertolasi, V., de Palo, M., Distefano, G., Jones, D., Modelli, A. & Olivato, P. R. (1995). *J. Phys. Chem.* **99**, 15011–15017.

Distefano, G., Dal Colle, M., Bertolasi, V., Olivato, P. R., Bonfada, O. & Mondino, M. G. (1991). *J. Chem. Soc. Perkin Trans. 2*, pp. 1195–1199.

Distefano, G., Dal Colle, M., de Palo, M., Jones, D., Bombieri, G., Del Pra, A., Olivato, P. R. & Mondino, M. G. (1996). *J. Chem. Soc. Perkin Trans. 2*, pp. 1661–1669.

Fleming, I. (1976). *Frontier Orbitals and Organic Chemical Reactions*, p. 209. Chichester: Wiley.

Frisch, M. J., Trucks, G. W., Schlegel, H. B., Scuseria, G. E., Robb, M. A., Cheeseman, J. R., Zakrzewski, V. G., Montgomery Jr, J. A., Stratmann, R. E., Burant, J. C., Dappich, S., Millam, J. M., Daniels, A. D., Kudin, K. N., Strain, M. C., Farkas, O., Tomasi, J., Barone, V., Cossi, M., Cammi, R., Mennucci, B., Pomelli, C., Adamo, C., Clifford, S., Ochterski, J., Petersson, G. A., Ayala, P. Y., Cui, Q, Morokuma, K., Malick, D. K., Rabuck, A. D., Raghavachari, K., Foresman, J. B., Ciosłowski, J., Ortiz, J. V., Stefanov, B. B., Liu, G., Liashenko, A., Piskorz, P., Komaromi, I., Gomperts, R., Martin, R. L., Fox, D. J., Keith, T., Al-Laham, M. A., Peng, C. Y., Nanayakkara, A., Gonzalez, C., Challacombe, M., Gill, O. M. W., Johnson, B. G., Chen, W., Wong, J. L., Andres, J. L., Head-Gordon, M., Replogle, E. S. & Pople, J. A. (1998). *GAUSSIAN98*. Revision A.6. Gaussian Inc., Pittsburgh PA, USA.

Gałdecki, Z., Kowalski, A. & Uszyński, L. (1995). *DATAPROC*, Version 9.0. Kuma Diffraction, Wrocław, Poland.

Gilli, G., Bellucci, F., Ferretti, V. & Bertolasi, V. (1989). *J. Am. Chem. Soc.* **111**, 1023–1028.

Gilli, P., Bertolasi, V., Ferretti, V. & Gilli, G. (1994). *J. Am. Chem. Soc.* **116**, 909–915.

Gómez-Sánchez, A., García Martín, M. G., Borrachero, P. & Bellanoto, J. (1987). *J. Chem. Soc. Perkin Trans. 2*, pp. 301–306.

Graczyk, P. R. & Mikołajczyk, M. (1994). *Topics in Stereochemistry*, edited by E. L. Eliel and S. H. Wilen, pp. 159–349. New York: Wiley.

Grossert, J. S., Ranjith, H., Dharmaratne, T., Cameron, T. S. & Vincent, B. R. (1987). *Can. J. Chem.* **66**, 2860–2869.

Hansch, C. & Leo, A. (1979). *Substituent Constants for Correlation Analysis in Chemistry and Biology*. Weinheim: Verlag Chemie.

Hasall, K. A. (1982). *The Chemstry of Pesticides. Their Metabolism, Mode of Action and Uses in Crop Protection*, p. 179. Wienheim: Verlag Chemie.

Hoffmann, R. (1971). *Acc. Chem. Res.* **4**, 1–9.

Hohenberg, P. & Kohn, W. (1964). *Phys. Rev. B*, **136**, 864–871.

Juaristi, E. & Cuevas, G. (1995). *The Anomeric Effect*. Boca Raton: CRC Press.

Kucsman, A. & Kapovits, J. (1985). *Organic Sulfur Chemistry. Theoretical and Experimental Advances*, edited by F. Bernardi, I. G. Csizmadia and A. Mangini, pp. 226–245. Amsterdam: Elsevier.

Kuma Diffraction (1991). *KM*-4 *User's Guide*, Version 3.2. Kuma Diffraction, Wrocław, Poland.

Lee, C., Yang, W. & Parr, R. G. (1988). *Phys. Rev. B*, **37**, 785–789.

Levy, M. (1979). *Proc. Natl. Acad. Sci. USA*, **76**, 6062–6065.

Mayer, I. (1986). *Int. J. Quantum Chem.* **29**, 477–483.

Molecular Simulations Inc. (1996). *DMOL User Guide*. Version 96.0. Molecular Simulations Inc., San Diego, USA.

Olivato, P. R., Guerrero, S. A. & Zukerman-Schpector, J. (2000). *Acta Cryst.* B**56**, 112–117.

Olivato, P. R., Mondino, M. G., Yreijo, M. H., Blanka, W., Bjorklund, M. B., Marzorati, L., Distefano, G., Dal Colle, M., Bombieri, G. & Del Pra, A. (1998). *J. Chem. Soc. Perkin Trans.* 2, pp. 109–114.

Roberts, J. D., Webb, R. L. & McElhill, A. (1950). *J. Am. Chem. Soc.* **72**, 408–411.

Rüchardt, Ch. & Beckhaus, H.-D. (1985). *Angew. Chem. Int. Ed. Engl.* **24**, 529–538.

Sheldrick, G. M. (1997a). *SHELXL*97. University of Göttingen, Germany.

Sheldrick, G. M. (1997b). *SHELXS*97. University of Göttingen, Germany.

Siemens (1989). *P*3, Version 2.0. Siemens Analytical X-ray Instruments Inc., Madison, Wisconsin, USA.

Siemens (1990). *XP*, Version 4.1. Siemens Analytical X-ray Instruments Inc., Madison, Wisconsin, USA.

Siemens (1991). *XDISK*, Version 4.20. Siemens Analytical X-ray Instruments Inc., Madison, Wisconsin, USA.

Singh, U. C. & Kollman, P. A. (1984). *J. Comput. Chem.* **5**, 129–145.

TRIPOS Associates Inc. (1996). *SYBYL*, Version 6.3. TRIPOS Associates Inc., St Louis, Missouri, USA.

Wolf, W. M. (1999a). *Acta Cryst.* C**55**, 469–472.

Wolf, W. M. (1999b). *J. Mol. Struct.* **474**, 113–124.

Zakrzewski, A. (1996). Private communication.

Zakrzewski, A. (1999). *Przemysł Chemiczny*, **78**, 17–19.

Zakrzewski, A. & Kacała, A. (1998). *Pestycydy*, **4**, 21–30.

62   W. M. Wolf · Sulfur-containing fungicides. II

Acta Cryst. (2001). B**57**, 54–62